

# Applications of deep learning to relativistic hydrodynamics

Hengfeng Huang,<sup>1,2</sup> Bowen Xiao,<sup>3</sup> Huixin Xiong,<sup>1</sup> Zeming Wu,<sup>1,2</sup> Yadong Mu,<sup>3,4,\*</sup> and Huichao Song<sup>1,2,5,†</sup>

<sup>1</sup>Department of Physics and State Key Laboratory of Nuclear Physics and Technology, Peking University, Beijing 100871, China

<sup>2</sup>Collaborative Innovation Center of Quantum Matter, Beijing 100871, China

<sup>3</sup>Institute of Computer Science and Technology, Peking University, Beijing 100080, China

<sup>4</sup>Center for Data Science, Peking University, Beijing 100871, China

<sup>5</sup>Center for High Energy Physics, Peking University, Beijing 100871, China

(Dated: July 6, 2022)

Relativistic hydrodynamics is a powerful tool to simulate the evolution of the quark gluon plasma (QGP) in relativistic heavy ion collisions. Using 10000 initial and final profiles generated from 2+1-d relativistic hydrodynamics VISH2+1 with MC-Glauber initial conditions, we train a deep neural network based on **stacked U-net**, and use it to predict the final profiles associated with various initial conditions, including MC-Glauber, MC-KLN and AMPT and TRENTo. A comparison with the VISH2+1 results shows that the network predictions can nicely capture the magnitude and inhomogeneous structures of the final profiles, and nicely describe the related eccentricity distributions  $P(\epsilon_n)$  ( $n=2, 3, 4$ ). These results indicate that deep learning technique can capture the main features of the non-linear evolution of hydrodynamics, showing its potential to largely accelerate the event-by-event simulations of relativistic hydrodynamics.

PACS numbers:

*Introduction* Deep learning is a machine learning technology employing deep neural networks as a tool. With the development of big data and powerful computing equipment, it has led to significant progresses in computer vision, speech recognition [1] and playing games [2]. Recently, deep learning has been implemented in various research areas in physics, including the search of gravitational lens[3, 4], identifying and classifying the phases of Ising model [5–7], solving the quantum many body problem [8, 9], etc. In high energy physics, it has been applied to the search of Higgs and exotic particles [10, 11], jet structure classification [12, 13], identifying the equation of state of hot QCD matter [14], etc.

In this paper, we will apply deep learning to relativistic hydrodynamics, which is a useful tool to simulate the macroscopic evolution of relativistic systems in high energy nuclear physics and astrophysics [15]. Relativistic hydrodynamics solves the transport equations of the energy momentum tensor and charge currents based on the conservation laws. In relativistic heavy ion collisions, it has nicely described and predicted various flow data of the quark-gluon plasma (QGP) [16, 17], which played an important role in the discovery of the strongly coupled QGP [18]. However, traditional hydrodynamic simulations are time consuming. For example, the calculation of various flow harmonics requires  $\sim 1000$  event-by-event hydrodynamic simulations, which takes  $\sim 500$  and  $\sim 10000$  cpu hours for the typical 2+1-d and 3+1-d simulations, respectively [17, 20]. Basically, relativistic hydrodynamics translate the initial conditions to final profiles through solving a set of non-linear differential equations. In this work, we will explore whether the deep neural network could capture the main features of the non-linear evolution of 2+1-d hydrodynamics, and the possibilities to accelerate the related event-by-event simulations.

*Relativistic hydrodynamics* In this paper, we focus on relativistic ideal hydrodynamics with zero viscosity and charge densities, which solves the transport equations of the energy momentum tensor  $T^{\mu\nu}$ :

$$\partial_\mu T^{\mu\nu} = 0 \quad (1)$$

where  $T^{\mu\nu} = (e+p)u^\mu u^\nu - pg^{\mu\nu}$ ,  $e$  is the energy density,  $p$  is the pressure, and  $u^\mu$  is the four velocity with  $u^\mu u_\mu = 1$ . With an assumption of longitudinal boost invariance, we solve the 2+1-dimensional hydrodynamic equations with an ideal EoS  $p = \frac{e}{3}$ , using the code VISH2+1 [19, 20][28]. The initial energy density profiles can be generated by some initial condition models, such as MC-Glauber [21, 22], MC-KLN [22, 23], AMPT [24] and TRENTo [25] with zero initial transverse flow velocity. We run VISH2+1 with three selected fixed evolution times  $\tau - \tau_0 = 2.0, 4.0$  and  $6.0$  fm/c ( $\tau_0=0.6$  fm/c) to obtain the energy momentum tensor  $T^{\tau\tau}(\tau, x, y)$ ,  $T^{\tau x}(\tau, x, y)$ ,  $T^{\tau y}(\tau, x, y)$  profiles at these times. For numerical accuracy, the time step and grid sizes of the simulations are set to  $d\tau = 0.04$  fm/c and  $dx = dy = 0.1$  fm, within a fixed transverse area of  $13 \text{ fm} \times 13 \text{ fm}$  that have been used to describe the typical QGP expansion in relativistic heavy ion collisions.

*Network design* For deep learning, the initial and final energy momentum tensor  $T^{\tau\tau}$ ,  $T^{\tau x}$ ,  $T^{\tau y}$  profiles from hydrodynamics are treated as initial and final image sets with  $261 \times 261$  pixels. In practice, we first run the event-by-event hydrodynamic simulations to obtain 10000 initial and final image sets, then use them to train the deep neural network, which aims at achieving nice predictions of the final energy density and flow velocity profiles for other input initial conditions.

The related network we adopted in this work is the **stacked U-net (sU-net)** [27], which is a variation of the traditional encoder-decoder network that could enhance

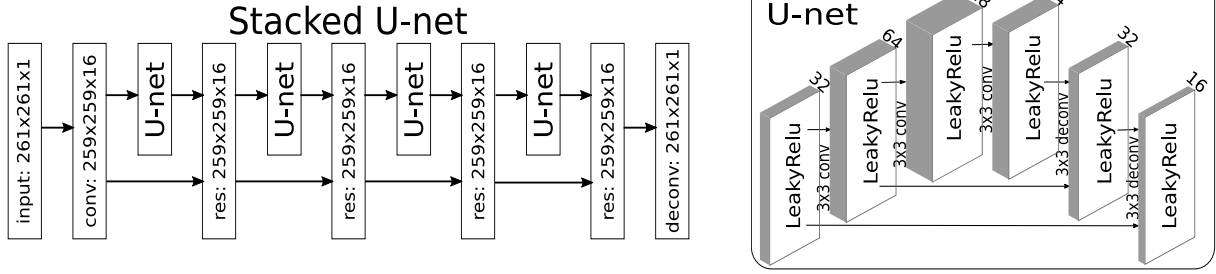


FIG. 1: An illustration of the encode-decode network, **stacked U-net**, which consists of the input and out layers and four residual U-net blocks. The right figure shows the U-net structure, and the depth of the hidden layer is written on the top of them.

gradient flow in the deeper part of the network during back propagation. Fig. 1 presents an intuitional view of the network structure. It consists of 4 serially connected U-net blocks with residual connections between them. Each U-net block has 3 convolution layers and 3 deconvolution layers. In each U-net block, the output of the first two convolution layers are also fed into the last two deconvolution layers respectively by concatenating the feature maps along the channel dimension. The activation function for all layers except for the output one is *Leaky ReLU*  $f(x) = \max\{x, 0.03x\}$ , while that for the output layer is *softplus*  $f(x) = \ln(1 + e^x)$  for  $T^{\tau\tau}$  mapping and  $f(x) = 1$  for  $T^{\tau x}$  and  $T^{\tau y}$  mapping. To make the network focus more on local patterns, we set the kernel size of all convolution and deconvolution layers to  $3 \times 3$ . The loss function of the network is *normalized MAE loss*  $Loss = \frac{|y_1 - y_0|}{|y_0|}$ , where  $y_1$  is the output of the network and  $y_0$  is the ground truth. We use the standard mini-batch stochastic gradient descent algorithm for optimization. The batch size for training is 16 and learning rate exponentially decays from  $10^{-3}$  to  $10^{-5}$ . Our code is built with TensorFlow and the training process runs for about 1 day on a machine with single NVIDIA Tesla P40 GPU, using 10000 “initial” and “final” profiles from VISH2+1 hydrodynamic simulations.

We have noticed that, although one trained **sU-net** can make nice predictions for shorter hydrodynamic evolution, it fails to accurately predict the final profiles of longer evolution time ( $\tau - \tau_0 > 4.0$  fm/c) from the initial profiles at  $\tau_0$  [26]. Considering that the evolving QGP system is highly non-linear and tends to smear-out its initial structures during longer evolution, we divide the whole evolution time  $\tau - \tau_0$  into  $n$  parts with equal time interval  $\Delta\tau$ :  $\tau - \tau_{n-1} \dots \tau_2 - \tau_1, \tau_1 - \tau_0$ . For each evolution part, we train an individual **sU-net** using the corresponding “initial” and “final” profiles from hydrodynamics. To predict the final profiles at  $\tau$  from initial profiles at  $\tau_0$ , we first use the trained **sU-net-1** to predict the profiles at time  $\tau_1$  and then use them as the initial conditions for **sU-net-2** to predict the profiles at time  $\tau_2$  and so on. In this way, the combined **sU-net**

series ( $i=1\dots n$ ) mimic the hydrodynamic evolution with much larger time step  $\Delta\tau$  that can not be managed by traditional hydrodynamic algorithm (In more detail, for the following evolution with  $\tau - \tau_0 = 6.0$  fm/c, we set  $n=3$  with  $\Delta\tau = 2.0$  fm/c). It also helps to significantly accelerate the related event-by-event hydrodynamic simulations. Please refer to the following long paper for more details [26].

*Results* As explained in the above text, we first use 10000 initial and final image sets from VISH2+1 with MC-Glauber initial conditions to train the combined **stacked U-net**, and then use the trained network to predict the final profiles from the initial profiles generated from MC-Glauber, MC-KLN, AMPT and TRento as tests. Fig. 2 presents a comparison between the results from VISH2+1 hydrodynamic evolution and the predictions from the network at  $\tau - \tau_0 = 2.0, 4.0, 6.0$  fm/c for 6 selected test cases. It shows that the well designed and trained network could nicely predict the final states, which captures the structures of the contour plots for both final energy density and flow velocity. It is impressive that, although the network is trained with the initial and final image sets associated with the MC-Glauber initial conditions, it could still nicely predict the final profiles of other initial conditions with different fluctuation patterns, as shown in panel (b), (d) and (f).

To further evaluate the predictive power of the network, we further calculate the eccentricity coefficients

$$\varepsilon_n = \frac{\int r dr d\phi r^n e(r, \phi) e^{in\phi}}{\int r dr d\phi r^n e(r, \phi)} \quad (n = 2, 3, 4) \quad (2)$$

for initial and final energy density  $e(r, \phi)$  profiles, which are quantities commonly used to evaluate the deformation and inhomogeneity of the QGP fireball in relativistic heavy ion collisions [17]. These values of  $\varepsilon_n$  ( $n=2, 3, 4$ ) for these 6 selected test cases are written in the related panels (a-f). From Fig. 2 and the calculated values of  $\varepsilon_n$  ( $n=2, 3, 4$ ), we have also noticed that differences between the hydrodynamic results and the network predictions increase for longer evolution time since the combined **sU-net** series tend to accumulate errors with more

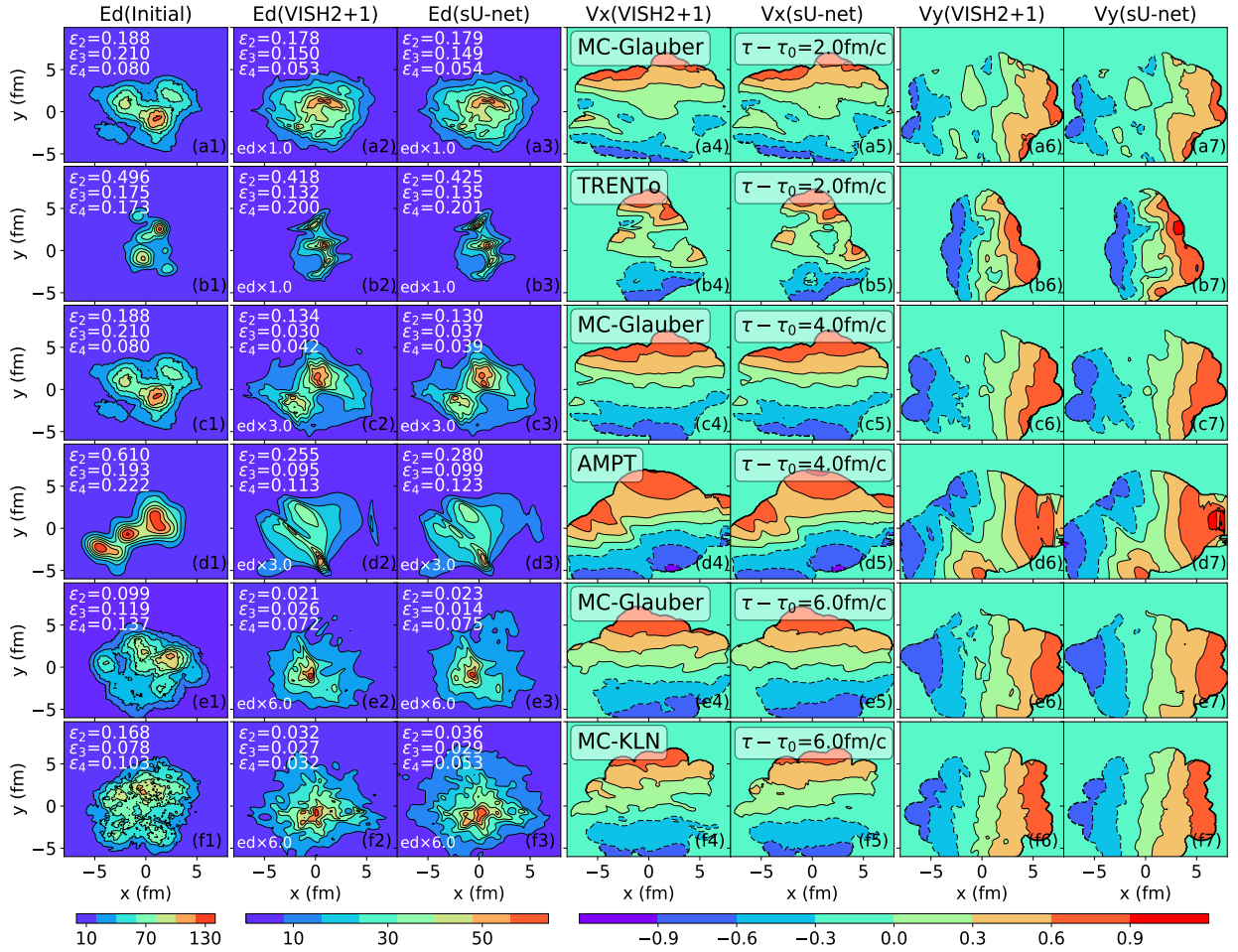


FIG. 2: Energy density and flow velocity profiles at  $\tau - \tau_0 = 2.0, 4.0, 6.0$  fm/c, calculated from VISH2+1 and predicted by the network for six test cases with initial profiles generated from MC-Glauber, MC-KLN, AMPT and TRENTo.

sU-net added. For details, please refer to [26].

Fig. 3 presents the eccentricity distributions  $P(\epsilon_n)$  for the energy density profiles at evolution times  $\tau - \tau_0 = 2.0$  fm/c, 4.0 fm/c and 6.0 fm/c, calculated from VISH2+1 and predicted from the network for 10000 tested initial profiles generated from MC-Glauber, MC-KLN, AMPT and TRENTo. For all these tested cases, the final eccentricity distributions  $P(\epsilon_n)$  ( $n=2, 3, 4$ ) from the network almost overlap with the ones from VISH2+1, which also obviously deviate from the initial eccentricity distributions  $P_0(\epsilon_n)$ .

We also find that, with the well trained network, the final state profiles can be speedily generated from the initial profiles. Compared with the 10-20 minute calculation time with traditional CPU for a single-event hydrodynamic evolution, the network takes several seconds to directly generate the final profile for different types of initial profiles with the P40 GPU, which shows the potential to significantly accelerate the realistic event-by-event hydrodynamic simulations in the near future.

*Conclusion and outlook* Using 10000 initial and final energy momentum tensor profiles from VISH2+1 hydro-

dynamics with MC-Glauber initial conditions, we successfully trained a deep neural network based on **stacked U-net**, and use it to predict the final profiles for different initial conditions, including MC-Glauber, MC-KLN, AMPT and TRENTo. A comparison with the VISH2+1 results showed that the network predictions could nicely capture the magnitude and inhomogeneous structures of the final profiles, which also nicely describe the related eccentricity distributions  $P(\epsilon_n)$  ( $n=2, 3, 4$ ). These results indicate that deep learning could capture the main feature of the non-linear evolution of hydrodynamics, which also shows the potential of largely accelerating the realistic event-by-event hydrodynamic simulations in relativistic heavy ion collisions.

Currently, our investigations mainly focus on mimicking the 2+1-dimensional hydrodynamic evolution with fixed evolution time, using the deep learning technique. For more realistic implementation to relativistic heavy ion collisions, it is worthwhile to explore the possibilities of mapping the initial profiles to the final profiles on the freeze-out surface with fixed energy density as well as

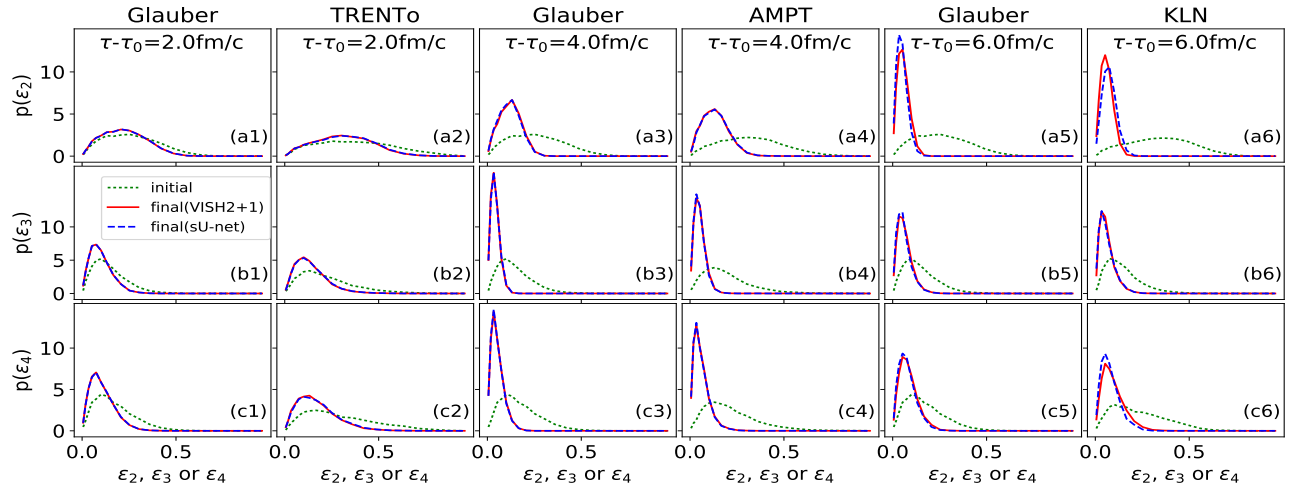


FIG. 3: Eccentricity distribution  $P(\epsilon_n)$  ( $n=2, 3, 4$ ), at  $\tau - \tau_0 = 2.0, 4.0, 6.0$  fm/c, calculated from VISH2+1 and predicted by the network for 100000 tested initial profiles generated from MC-Glauber, MC-KLN, AMPT and TRENTo.

extending the related investigations to 3+1-dimensional simulations.

### ACKNOWLEDGMENTS

We thanks the discussions from L. G. Pang and K. Zhou. H. H, H. X. Z. W. and H. S. are supported by the NSFC and the MOST under grant Nos.11435001, 11675004 and 2015CB856900. B. X. and Y. M. are supported by NSFC under grant no. 61772037.

\* Electronic address: myd@pku.edu.cn

† Electronic address: huichaosong@pku.edu.cn

- [1] Y. LeCun, Y. Bengio and G. Hinton, *Nature* **521**, 436 (2015).
- [2] D. Silver *et al.*, *Nature* **529**, 484 (2016).
- [3] C. E. Petrillo *et al.*, *Mon. Not. Roy. Astron. Soc.* **472**, 1129 (2017).
- [4] Y. D. Hezaveh, L. Perreault Levasseur and P. J. Marshall, *Nature* **548**, 555 (2017).
- [5] J. Carrasquilla and G. R. Melko, *Nature Phys.* **13**, 431 (2017).
- [6] E. P. L. van Nieuwenburg, Y. H. Liu, S. Huber, *Nature Phys.* **13**, 435 (2017).
- [7] P. Broecker, J. Carrasquilla, R. G. Melko and S. Trebst, *Sci. Rep.* **7**, 8823 (2017).
- [8] G. Garleo and M. Troyer, *Science* **355**, 602 (2017).
- [9] X. Gao, L. M. Duan, *Nature Commun.* **8**, 662 (2017).
- [10] P. Baldi, P. Sadowski and D. Whiteson, *Nature Commun.* **5**, 4308 (2014).
- [11] P. Baldi, K. Cranmer, T. Faucett, P. Sadowski and D. Whiteson, *Eur. Phys. J. C* **76**, no. 5, 235 (2016).
- [12] P. Baldi, K. Bauer, C. Eng, P. Sadowski and D. Whiteson, *Phys. Rev. D* **93**, no. 9, 094034 (2016).
- [13] P. T. Komiske, E. M. Metodiev and M. D. Schwartz, *JHEP* **1701**, 110 (2017).
- [14] L. G. Pang, K. Zhou, N. Su, H. Petersen, H. Stocker and X. N. Wang, arXiv:1612.04262 [hep-ph].
- [15] L.D. Landau and E.M. Lifshitz, *Course of Theoretical Physics Volume 6, Fluid Mechanics*, Elsevier, 2nd edition (1987).
- [16] P. Huovinen, in *Quark Gluon Plasma 3*, edited by R. C. Hwa and X. N. Wang (World Scientific, Singapore, 2004), p. 600 P. F. Kolb and U. Heinz, *ibid.*, p. 634.
- [17] U. Heinz and R. Snellings, *Annu. Rev. Nucl. Part. Sci.* **63**, 123 (2013); C. Gale, S. Jeon and B. Schenke, *Int. J. Mod. Phys. A* **28**, 1340011 (2013); H. Song, *Nucl. Phys. A* **904-905**, 114c (2013); H. Song, Y. Zhou and K. Gajdosova, *Nucl. Sci. Tech.* **28**, no. 7, 99 (2017).
- [18] M. Gyulassy and L. McLerran, *Nucl. Phys. A* **750**, 30 (2005); B. Muller and J. L. Nagle, *Ann. Rev. Nucl. Part. Sci.* **56**, 93 (2006); B. Muller, J. Schukraft and B. Wyslouch, *Ann. Rev. Nucl. Part. Sci.* **62**, 361 (2012).
- [19] H. Song and U. W. Heinz, *Phys. Rev. C* **77**, 064901 (2008).
- [20] C. Shen, Z. Qiu, H. Song, J. Bernhard, S. Bass and U. Heinz, *Comput. Phys. Commun.* **199**, 61 (2016).
- [21] M. L. Miller, K. Reygers, S. J. Sanders and P. Steinberg, *Ann. Rev. Nucl. Part. Sci.* **57**, 205 (2007).
- [22] T. Hirano and Y. Nara, *Phys. Rev. C* **79**, 064904 (2009).
- [23] H. J. Drescher and Y. Nara, *Phys. Rev. C* **75**, 034905 (2007); *Phys. Rev. C* **76**, 041903(R) (2007).
- [24] L. Pang, Q. Wang and X. N. Wang, *Phys. Rev. C* **86**, 024911 (2012); H. j. Xu, Z. Li and H. Song, *Phys. Rev. C* **93**, no. 6, 064905 (2016).
- [25] J. S. Moreland, J. E. Bernhard and S. A. Bass, *Phys. Rev. C* **92**, no. 1, 011901 (2015).
- [26] H. Hunag, *et. al.*, in preparation.
- [27] K. He, X. Zhang, S. Ren and J. Sun, *Proc. IEEE Comput. Soc. Conf. Comput. Vis. Pattern Recognit.*, p. 770 (2015).
- [28] In  $(\tau, x, y, \eta)$  coordinate ( $\tau = \sqrt{t^2 - z^2}$  and  $\eta = \frac{1}{2} \ln \frac{t+z}{t-z}$ ), the energy density and pressure from 2+1-d hydrodynamics are longitudinal boost-invariant without a dependence on  $\eta$ ,  $e=e(\tau, x, y)$  and  $p=p(\tau, x, y)$ . Correspondingly, the four flow velocity are expressed as  $\gamma_{\perp}(1, v^x(\tau, x, y), v^y(\tau, x, y), 0)$  with  $v^{\eta} = 0$  [16].